Markov Decision-Based Pilot Optimization for 5G V2X Vehicular Communications

Yan Yang, *Member, IEEE*, Shuping Dang, *Member, IEEE*, Yejun He, *Senior Member, IEEE*, and Mohsen Guizani, *Fellow, IEEE*

***Abstract*—This paper proposes a Markov decision process (MDP)-based pilot placement optimization approach for the radio access in 5G vehicle to everything communications to support Internet of Vehicles applications. The optimal placement problem of pilot symbols is based on a typical pilot-assisted frequency-division multiplexing transmission and simplified to a finite state-space representation. We propose and formulate a finite MDP so as to determine an appropriate pilot pattern from a set of candidate pilot configurations. Also, an enhanced pilot placement scheme is developed to reduce the complexity for solving the formulated MDP problems. Furthermore, we derive analytical expressions of the mutual information, which to some extent allow us to jointly evaluate the dynamics of the channel state in time and frequency domains. Numerical results generated by Monte Carlo simulations show that the proposed pilot optimization policy is capable of improving the channel estimation in fast time-varying vehicular channels, and the mutual information-based measurement criteria can yield more accurate evaluations in fast time-varying vehicular channels than other conventional schemes.**

***Index Terms*—Fast time-varying channel, fifth generation (5G) vehicle to everything (V2X), Markov decision process (MDP), mutual information, pilot optimization.**

I. Introduction

VEHICLE to everything (V2X) is considered as a critical component of fifth generation (5G) networks, which aims to satisfy high requirements in terms of reduced latency, increased reliability, and higher throughput under higher mobility and connectivity density. V2X directly connects vehicles to everything including to vehicle (V2V), to pedestrians (V2P), and to roadway infrastructure (V2I), and to the network. The key features of V2X focus on ultrareliable and low latency communication for safety-critical use cases, e.g., hazard warning, intersection assistance, and automated and/or autonomous driving [1]–[4]. Although the IEEE 802.11p Standard has already defined a collection of physical layer (PHY) specifications and media access control to support wireless access in vehicular environments, it was not realized for the lack of infrastructure, a carrier sense multiple access with collision avoidance can face some challenges when guaranteeing strict reliability levels and ensuring the network scalability as the load increases [5]. From this perspective, 5G V2X seems to be better for automotive industry because of its infrastructure, tremendous capacity, and added direct device-to-device (D2D) communication services [6].

In an effort to provide ubiquitous access, 5G networks shall enable vehicles to accommodate different types of V2X message deliveries to support intelligent transportation systems, where all vehicles and infrastructure systems are interconnected with each other. For this reason, connected vehicles are becoming the next frontier for Internet of Things, whereas the original concept of vehicular ad-hoc networks is being transformed into a new concept called the Internet of Vehicles (IoV) [7]. Accordingly, continuous 5G V2X technology evolution is required to support high-reliability and low-latency radio access for critical messages even in the high density IoV systems.

Since orthogonal frequency-division multiplexing (OFDM) is currently one of the most mature modulation technologies adopted in the PHY of 5G related standards, the use of pilot symbols is an effective technique to capture channel variations for both downlink and uplink transmissions [8]. In traditional OFDM systems, as well as multiple input multiple output (MIMO) systems, it has been proven that pilot symbols play a crucial role in channel estimation, receiver adaptation, and optimal decoding. In this sense, a suitable alternative of pilot placement would have a significant impact on the overall performance of wireless communication systems [9]. However, most standards define a fixed number of pilots to be deployed, but do not specify the optimal pilot allocation in accordance with different conditions of wireless channels, e.g., multipath propagation, obstructions, mobility of vehicles, etc. This would lead to unnecessary pilot overhead under

Manuscript received July 1, 2018; revised August 6, 2018; accepted August 19, 2018. Date of publication August 27, 2018; date of current version February 25, 2019. This work was supported in part by the Research Task of the State Key Laboratory of Rail Traffic Control and Safety under Grant RCS2017ZT010, in part by the China Scholarship Council, in part by the Research Task of China Railway Corporation under Grant 2016X009-A, in part by the National Natural Science Foundation of China under Grant 61372077/61871433, in part by the Shenzhen Science and Technology Programs under Grant JCYJ20170302150411789 and Grant JCYJ20170302142515949, and in part by the Guangzhou Science and Technology Program under Grant 201707010490. *(Corresponding author: Yan Yang.)*

Y. Yang is with the State Key Laboratory of Rail Traffic Control and Safety, Beijing Jiaotong University, Beijing 100044, China (e-mail: yyang@bjtu.edu.cn).

S. Dang was with the Department of Engineering Science, University of Oxford, Oxford OX1 3PJ, U.K. He is now with the Research and Development Center, Guangxi Huanan Communication Company, Ltd., Nanning 530007, China (e-mail: shuping.dang@hncom.ac.cn).

Y. He is with the Shenzhen Key Laboratory of Antenna and Propagation, College of Information Engineering, Shenzhen University, Shenzhen 518060, China (e-mail: heyejun@126.com).

M. Guizani is with the Electrical and Computer Engineering Department, University of Idaho, Moscow, ID 83844 USA (e-mail: mguizani@ieee.org).

Digital Object Identifier 10.1109/JIOT.2018.2867334

good channel conditions and performance degradation under unsatisfactory channel conditions. In practice, V2X operates in different channel conditions: 1) in low mobility and strong line of sight scenario, the channel is flat in time and frequency, e.g., V2P and 2) in high mobility and strong scattering environment, the channel exhibits a strong frequency selectivity and fast time-varying fading, e.g., V2V and V2I. In high mobility scenarios, V2X is susceptible to severe Doppler shift and higher multipath delay spread in high mobility scenarios, and channel estimation would be a challenging task in regards to providing ultrahigh throughput, low latency and high reliability in fast fading vehicular environments [10].

The channel estimation performance is affected by pilot symbols and their placement significantly. In brief, the pilot optimization would be understood as a strategy for, where and/or how often the pilot tones are inserted in the data stream. An overview of pilot-assisted transmission on the general model, design criteria and signal processing can be found in [9]. For pilot-assisted OFDM systems, the optimal pilot placement design can be classified into two categories. The first category is to find optimal pilot placement patterns for channel estimation, aiming at maximizing channel capacity, and guaranteeing a prescribed transmission performance and/or spectral efficiency under the constraint of pilot power and spacing. In long term evolution and the latest digital terrestrial television standards, the use of pilots is an effective technique for channel estimation, and higher flexibility in pilot design is suggested in new 5G air interface for high speed and high throughput V2X scenarios (e.g., video to and from automobiles) [11]. The second category seeks the optimal pilot placement strategies for joint estimation of carrier frequency offset (CFO) and channel impulse response (CIR).

Several common design criteria of channel estimators, e.g., mean squared error (MSE) and minimum mean square error (MMSE), have been well studied, in which bit error rate (BER) or symbol error rate (SER) is considered as the most appropriate performance metric [9], [12]–[16]. While [17] showed that the optimal pilot sequences were equipowered, equispaced and phase shift orthogonal, a number of existing papers dealt with pilot optimizations based on regular periodic placements. Dong *et al.* [18] proved that periodic pilot placements can minimize the maximum steady-state channel MMSE, and showed that the superimposed scheme provides a better tracking ability than that of the single pilot RPP scheme (RPP-1) scheme in fast fading environments. In [13], the number of pilots, placement of pilot symbols and transmitted pilot power were optimized to minimize SER over Rayleigh fading channels. Ma *et al.* [12] proposed a training pattern for estimating CFO and MIMO frequency-selective channels and proved that hopping pilots from block to block can achieve the full acquisition range of CFO, where the impact of the Doppler-induced CFO and/or mismatch between transmit receive oscillators were taken into account.

To improve the spectral efficiency of OFDM systems, the studies of adaptive pilot placement, including the use of virtual subcarriers (also known as null subcarriers) data-aided channel estimation, have been continuously received much attention [15], [19]–[21]. Karami and Beaulieu [22] proposed an optimal pilot parameter adjustment approach for rapidly fading channels, and designed a joint adaptive power loading and pilot spacing algorithm to maximize the average mutual information between the input and output of OFDM systems. Using virtual pilots to obtain the channel estimation was first proposed in [19], where the extra data symbols (also known as virtual pilot tones) are exploited to improve the performance of channel estimation. The adaptive pilot optimization is another attractive technique to mitigate the effects of time-varying channel. Karami *et al.* [21] proposed a suboptimum pilot symbol assisted adaptive modulation scheme, and a suboptimum design was used to address optimum power and rate allocation based on available imperfect channel state information.

Recently, the reuse of the same pilot resource and the dynamic pilot resource scheduling techniques and new OFDM pilot waveform design for 5G outdoor ultra-dense network were proposed [23], [24], and results in [23] showed that the dynamic pilot scheduling scheme had a higher probability of successfully rescheduling users in high mobility environments. Chen and Chung [24] designed a new OFDM pilot waveform for quasi-static channel estimation and provided extremely high spectral compactness by suppressing spectral sidelobes. The problem of pilot parameter optimization for high-mobility OFDM channels was investigated in [25], and the authors dealt with the nonlinear optimization problem of pilot sequence design to minimize the MSE of the LMMSE channel estimate. For fast time-varying vehicular channel estimation, the more frequently pilot symbols are transmitted, the better the estimation and tracking, and the more robust the receiver will be [9], [26]. Yet it is not possible to allocate a large number of pilot subcarriers due to spectrum loss, since pilot symbols *per se* do not carry information. In this regard, a sparse pilot design within multiple OFDM symbols should be taken into account.

In this paper, we consider an OFDM-based 5G V2X communication technology for future IoV applications. Our idea is to perform the pilot selection based on the results of Markov decision process (MDP), so that the optimal pilot placement can be used to capture the channel variations. It will be shown that the proposed method can achieve significant performance gains in nonstationary vehicular channels. While many studies of MDP solutions have appeared in the literature for adaptive resource allocation, video scheduling, and so on [27]–[29], a corresponding MDP expression model is needed to handle different problems, and most of these works have focused on finding a specific decision-making process. In this paper, we followed these general methods. The goal of the pilot placement optimization is to obtain optimal pilot patterns with low complexity, and to combat the effects of the fast time-varying channel. Since previous works have shown that equipowered pilot sequences lead to better performance, we only consider the pilot pattern with equispaced and equipowered pilot tones. The main contributions of this paper are given as follows.

1) We exploit an MDP-based pilot optimization approach for fast time-varying channel estimation. By specifying the dynamics of the channels with a finite state space, we then propose a finite MDP solution, while the decision problem can be solved in the feasible policy space.

We further develop a linear programming approach to solve the MDP for optimal pilot selection policy. We propose an enhanced pilot pattern design scheme for channel estimation, and the new scheme is capable of achieving desirable complexity-performance tradeoffs.

2) We develop a protocol-specific mechanism to support the information exchange of the pilot pattern directly among vehicles and between vehicles and roadside units (RSUs). The main advantage is that the notification of updating pilot pattern can be transmitted at a minimum latency and the processing overhead is thereby negligible.
3) To obtain the measurement criteria of MDP, we derive analytical expressions of mutual information to jointly evaluate the dynamics of the channel. By using the value iteration algorithm, an optimum pilot pattern can be determined for channel estimation.
4) Moreover, we investigate the impact of pilot placement strategies in time and frequency domains, and the numerical results show that the proposed pilot placement strategies can effectively track the fast time-varying channels and enhance the estimation accuracy of channel estimator.

The rest of this paper is organized as follows. In Section II, we describe the OFDM-based 5G V2X transmission and the pilot optimization model. In Section III, we consider the complexity tradeoffs of MDP, enhanced pilot patterns design and investigate the optimal pilot placement for channel estimation. In Section IV, we propose a mutual information assessment criterion and detail the optimization method based on MDP. Numerical results are presented and discussed in Section V, and this paper concludes in Section VI.

II. Problem Formulation

A. OFDM-Based 5G V2X Transmission

Consider a pilot-assisted OFDM-Based 5G V2X communication system that employs N subcarriers, where the time-frequency grid is equipped with N_p pilot subcarriers and N_d data subcarriers. For the kth transmitted data vector $\mathbf{x}(n;\ k) = [x(0; k), x(1, k), \ldots, x(N-1; k)]$, it is modulated by the inverse discrete Fourier transform (DFT) onto N parallel subcarriers, and the time-domain transmitted signal can be written as

$$x_t(n;\ k) = \sum_{l=0}^{N-1} x(l; k) e^{j2\pi ln/N}, \quad n = 0, 1, \ldots, N-1. \tag{1}$$

Suppose $x_t(n;\ k)$ is transmitted over a L-tap multipath channel with the transfer function $h(n;\ k)$. The signal at the receiver front-end can be expressed as

$$y_t(n;\ k) = x_t(n;\ k) \oplus h(n;\ k) + w(n;\ k) \tag{2}$$

where $\oplus$ denotes convolution; $w(n;\ k)$ is the additive white Gaussian noise (AWGN) and $h(n;\ k)$ is the CIR. Generally, the channel response $h(n;\ k)$ can be represented as $h(n;\ k) = \sum_{i=0}^{L-1} h_i e^{j\omega_{i,k}} \delta(\tau - \tau_{i,k})$, where $\omega_{i,k} = 2\pi f_{D_{i,k}} Tn/N, f_{D_{i,k}}$ is the ith path Doppler frequency shift; τ is delay spread index; T is the sample period, and $\tau_{i,k}$ is the ith path delay normalized by the sampling time. Once the DFT at the receiver with coherent detection can be performed correctly, the cyclic prefix is removed. Then, the received data vector $\mathbf{y}(n;\ k)$, can be demodulated by an unitary $N \times N$ DFT matrix $\mathbf{F}$ with element $F_{p,q} = 1/\sqrt{N}\exp^{j2\pi pq/N}$.

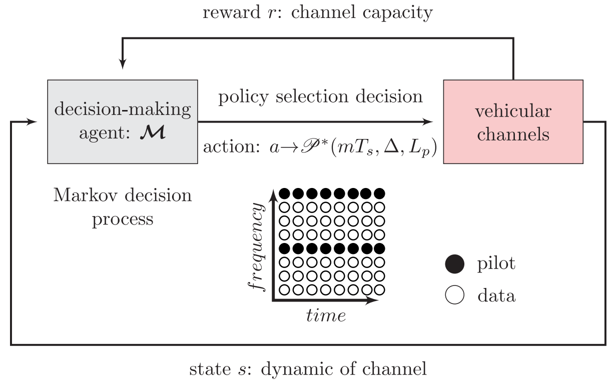

Fig. 1. OFDM pilot optimization model based on MDP.

Consider that the intersubcarrier interference (ICI) only comes from adjacent subcarriers. We can write the jth subcarrier of the kth received signal at the subcarrier level, in the form as

$$Y^{(j)}(n;\ k) = H^{(j)}(n;\ k) X^{(j)}(n;\ k) + \mathrm{ICI}^{(j)} + W^{(j)}(n;\ k) \tag{3}$$

where $H^{(j)}(n;\ k)$ is the channel frequency response (CFR); $X^{(j)}(n;\ k)$ is the frequency domain transmitted signal; $\mathrm{ICI}^{(j)}$ is the additive carriers interference component on the jth subcarrier, and $\mathrm{ICI}^{(j)} = \sum_{i=-j,\, i\neq 0}^{N-1-j} H^{(j+i)}(n;\ k) X^{(j+i)}(n;\ k)$ $i \leq |i_{\max}|$ i is the index of the interference subcarrier; $i_{\max}$ is the maximum number of the interference subcarriers; $W^{(j)}(n;\ k)$ denotes the noise term. For clarity, (3) can also be rewritten in the form of matrix as

$$\mathbf{Y}(n;\ k) = \mathbf{H}(n; k)\mathbf{X}(n; k) + \mathbf{W}(n;\ k) \tag{4}$$

where $\mathbf{H}(n;\ k)$ is the CFR matrix containing the multiplicative channel gain of the kth subchannel on its diagonal and the residual ICI terms on its nondiagonal entries, and $\mathbf{W}(n;\ k)$ is an independent and identically distributed (independent identically distributed) AWGN vector.

B. MDP-Based Pilot Placement Optimization

Fig. 1 illustrates the pilot optimization model, where an MDP decision-maker $\mathcal{M}$ is employed to determine the optimal pilot placement. The basic consideration is that the decision-maker $\mathcal{M}$ is designed to solve the optimal pilot placement according to the dynamic of the channel. Corresponding to a decision-maker $\mathcal{M}$, the vehicular channel is associated with a specific state s, and the goal of action a is to properly select control policy (i.e., optimal pilot placement) to adapt variant channels. Theoretically, when the channel state changes from a state s_i to another state s_j, the decision-maker $\mathcal{M}$ should choose an appropriate pilot placement $\mathscr{P}$ from a set of feasible decision options. In this paper, the constraint of the optimal pilot placement strategy $\mathscr{P}^*$ is defined as an objective function (rewards: r) that maximizes the system capacity.

Generally, pilot symbol spacing, power, and rate allocations are sufficient to characterize a pilot placement. Let T_s be the OFDM symbols duration, mT_s be the pilot spacing in time grid, and Δ be the pilot spacing in frequency grid. We can denote a set of pilot locations in an OFDM symbol by a three-tuple $\mathscr{P}(mT_s, \Delta, L_p)$, where L_p is the first location index of pilot subcarrier in frequency grid.

Strictly speaking, the channel statistics vary on a continuous scale, which means infinite channel state. For simplify, channel state can be viewed as a finite set of states (maximum number of resolvable multipath components, maximum Doppler shift, path delay, etc.), and the dynamics of the channels can be approximately specified by a finite state space. Accordingly, the state space of $\mathcal{M}$ can also be viewed as finite. In practice, since the number of orthogonal pilot sequences is limited, a unique pilot structure is only utilized to reflect an aggregated channel state. Based on this finite state space constraint, we formulate the pilot optimization problem as an optimal decision policy to identify the best way that pilot symbols can be multiplexed into the data stream, including pilot symbol spacing, power and rate allocations.

Typically, an MDP formulation $\mathcal{M}$ can be characterized by the tuple $\{\mathcal{T}, \mathcal{S}, \mathcal{A}, \mathcal{P}, \mathcal{R}\}$, where $\mathcal{S} = \{s_1, s_2, \ldots, s_n\}$ is a state space (i.e., channel state space) and $\mathcal{A} = \{a_1, a_2, \ldots, a_n\}$ is an action space that assigns the chosen action a in state s; $\mathcal{P} = \mathcal{P}_a(s, s')$ is the transition probability from current state s moving into a new state s', and $\mathcal{R} = \mathcal{R}_a(s, s')$ is the corresponding reward received by the system [30]. The objective of MDP is to find a policy $\pi : \mathcal{S} \rightarrow \mathcal{A}$, which maximizes the expected reward. Based on that, the pilot placement optimization process can be preliminarily described as follows.

1) $\mathcal{S}$ is a finite set of states, which can be assigned by the product of the channel state $h = \{h_1, h_2, \ldots, h_L\}$, and the optimal pilot control policy π is designed to receive a maximization of the reward $\mathcal{R}$. In our case, this maximization problem of $\mathcal{R}$ is equivalent to maximizing the channel capacity $\mathcal{C}$.
2) Without sacrificing the system capacity, we consider the following constraints on the feasible policy space π: the density of pilot symbols within an OFDM block is fixed and the pilots are spaced uniformly within each OFDM symbol. In this way, the selected pilot placement would not sacrifice the system capacity.
3) In each decision epoch, we calculate the cumulative reward function $\mathcal{R}_a(s, s')$ based on the current action a_m. Once the maximum $\mathcal{R}_a(s, s')$ is received, a new action will be terminated and otherwise, a new action a_n will be activated to choose the optimal pilot pattern $\mathscr{P}^*$.

In general, the typical channel fading process can be modeled as a first-order Gauss–Markov process [31]. In typical V2X (e.g., V2V and V2I) communication scenarios, the radio link, could be characterized to be time-varying and nonstationary [10]. Taking the effects of channel variance in time and frequency domains into account as a whole, both CIR and CFR can be modeled as

$$h(n;\ k) = \alpha h(n; k-1) + e(n; k-1) \tag{5a}$$

$$H(n;\ k) = \alpha H(n; k-1) + E(n; k-1) \tag{5b}$$

where $e(n; k-1)$, $E(n; k-1)$ are zero-mean Gaussian random noise, and $H(n;\ k)$ is CFR. In addition, the coefficients $\alpha \in [0, 1]$ show how quickly the channel changes in time and frequency domain (a small α corresponds to fast fading, while a large one refers to slow fading).

From (5a) and (5b), the dynamics of fast time-varying channels in time and frequency domains can be characterized. In this way, different physical parameters, e.g., the coherence time, delay spread, and Doppler spread can be used to describe the dynamics of channels. In this paper, we aim to find an optimum pilot placement that minimizes the MSE of the channel estimator, and a certain pilot placement pattern can be determined by solving a finite MDP problem. From the viewpoint of information theory, the channel capacity $\mathcal{C}$, as a natural performance evaluation metric, provides an accurate evaluation on system performance. Thus, the optimum pilot placement can be determined by maximizing the system capacity with a low cost.

In general, the channel dynamics can be characterized by their statistics based on physical propagation parameters, such as time spread and/or frequency spread [32]. We define the channel parameter sets χ and ψ associated with the channel parameters in the time and frequency domains, respectively, in which $\chi = \{\mathrm{PL}, \tau\}$ and $\psi = \{A, \Omega_D\}$, i.e., PL (path loss coefficient), τ (path delay), A (power spectrum), and Ω_D (delay-Doppler spectrum). According to the Shannon information capacity theorem, the capacity of fading channels is limited by the available transmit power and bandwidth. For a constant transmit power and bandwidth, the channel propagation condition can greatly impact the achievable system capacity. From (2), one can see that the received signal model is described as a function of the amplitude, delay and Doppler shifts, i.e., the channel capacity depends on the channel parameters, and as has a greater impact on spectral efficiency. In this paper, the pilot optimization is defined as to make an appropriate pilot pattern. We consider the sum of ergodic capacity as the optimization objective. For a given channel condition u ($u \in \{\chi, \psi\}$), the decision problem for the optimal pilot placement is to maximize the upper bound on the achievable capacity, which can be expressed as

$$\max_{u \in \{\chi, \psi\}} \mathcal{C}(u), \text{ s.t. } \Lambda(a) = \sum_i \lambda(a_i) < \kappa \tag{6}$$

where $\mathcal{C}(u)$ is the channel capacity (objective function) associated with the channel condition u; Λ is the total cost associated with a set of actions a; λ is the immediate cost with action a_i, and κ is a given minimum cost [30].

Based on (6), the optimum pilot placement would be viewed as a scheduling policy that seeks to maximize the channel capacity $\mathcal{C}(u)$. The objective of this paper is to employ an MDP-based policy to obtain the optimum pilot placement for better channel estimation in V2V and/or V2X communications. Typically, the feature of MDP can be defined by a tuple $(\mathcal{T}, \mathcal{S}, \mathcal{A}, \mathcal{P}, \mathcal{R})$, where $\mathcal{T}$, $\mathcal{S}$, $\mathcal{A}$, $\mathcal{P}$, and $\mathcal{R}$ are sets of decision epochs, system states, available actions, state and action dependent immediate reward, and state and action dependent transition probabilities [30]. The main idea for performing the optimization in this paper is based on the fact that the optimal placement of pilot symbols can be solved by tracking the fast time-varying channels. The determination of the optimum pilot placement by directly using an MDP formulation would not be possible, since the state space of the vehicular channels would be infinite in practice. We consequently consider a reasonable approximation, i.e., the number of possible channel state space associated with pilot placement is finite. By applying this constriction, the pilot placement policy is equivalent to solving an MDP on a finite-state set, which represents the dynamics of the channel in time and frequency domains.

In this paper, since the pilot placement affects BER performance, we optimize the pilot placement for MMSE channel estimation to minimize BER. We can rewrite (6) as

$$\begin{aligned} &\arg\max_{u\in\{\chi,\psi\}} && \mathcal{C}(\mathscr{P})|_u \\ &\text{s.t.} && \max\{\mathcal{R}_\pi\}, \quad \pi = \left\{d_1^*, d_2^*, \ldots, \right\} \end{aligned} \tag{7}$$

where $\mathcal{R}_\pi = \sum_i \boldsymbol{r}_i(s_i, a_i) - \Lambda(a)$ is the total reward associated with the immediate reward $\boldsymbol{r}(s, a)$ and π is the policy associated with a set of optimal decisions d_i^*, $d_i^* \in \mathcal{D}$. Once the optimal $\mathscr{P}^*$ is determined, the estimates of CIR at the pilot position $\hat{h}_p$ can be obtained by $\min_{h\in\mathcal{S}} |h - \hat{h}_p|^2, \forall\ \mathcal{S}$. Similarly, (7) can be solved by the exhaustive search algorithm, but it would lead to a high complexity by searching all possible combinations of pilot positions.

III. Enhanced Pilot Pattern Design for Channel Estimation

Considering that a large state/action space would make it difficult to solve an MDP problem, this section investigates a systematic tradeoff between performance and complexity. We develop an enhanced pilot pattern design scheme for channel estimation, which leads to a lower complexity and is capable of achieving compatibility with existing standards.

A. Performance-Complexity Tradeoffs of MDP

The existing pilot optimization methods for OFDM, including convex and adaptive optimization methods, etc., usually tend to search the best pilot placement over all possible pilot patterns. For fast varying vehicular channels, however, it might be difficult to assign an optimal pilot pattern for each channel state, and thereby it is highly likely that there exist a large number of pilot patterns which are not suitable for assignment. Although more pilot patterns might achieve a more accurate channel estimation, it would be unattractive for practical applications, since the computation of an optimal policy is very costly and causes another major drawback of capacity loss. Therefore, we have the following complexity restrictions.

1) The vehicular channels are specified with finite state space $\mathcal{S}$. Although vehicular channel states are dynamic and infinite in reality, it is not necessary to assign different pilot patterns to each channel state
2) The policy space is finite. Conventionally, the value iteration algorithm can be simplified, and would converge to the global optimum in a few number of iterations.

B. Enhanced Pilot Patterns Design

With the aforementioned complexity tradeoffs, a small number of pilot placements could be feasible to carry out channel estimation in time-varying OFDM systems. Therefore, the exhaustive search algorithm can be avoided. For a given number of subcarriers N and pilot spacing Δ, we assume that the pilot space in the frequency axis starts with variable location index L_p, and thus the maximum number of pilot patterns can be determined. Most of the wireless systems adopt a fixed pilot pattern for data detection purposes. It could constitute an unnecessary overhead under good channel conditions, whereas the performance degradation could occur under unsatisfactory channel conditions. This suggests that an appropriate pilot arrangement should be adaptively adjusted based on varying channel conditions.

Fig. 2 shows three groups of the pilot design with regular periodic placements with the same pilot density, which aims to capture channel variations for different vehicular communication conditions. Pattern set 0 represents a basic pilot placement, whereas patterns set 1 and 2 represent two enhanced pilot placements. In this paper, pattern set 0 is designed for low mobility scenarios, by which N OFDM subcarriers are in use (N_d subcarriers used for data transmission and N_p subcarriers used as pilots. Pattern set 1 is suitable for excess mobility scenarios with high Doppler shifts, $2 \times N_p$ pilot symbols are multiplexed into the data stream within two OFDM symbol periods. Pattern set 2 is suitable for high mobility with high delay spread, where the pilot symbols are interlaced in the time axis. Because the percentage of pilot symbols in each pilot pattern set is not changed in the time-frequency resource grid, thus, it would not cause any capacity loss.

To yield accurate channel estimates, we exploit a virtual pilot-assisted method as described in [15] and [19]. The characteristics of virtual pilot can be obtained as those subcarriers, where data have been detected without any error, with the highest probability [19]. We follow this approach, and the virtual pilots in this paper are identified as the data subcarriers between two successive pilot clusters, as shown in Fig. 2. With the aid of virtual pilots, the use of enhanced pilot patterns is equivalent to adding extra pilot symbols, so that the pilot subcarrier density could be viewed as approximately doubled. Clearly, it is useful to combat fast time-varying fading in vehicular channels. In the next section, we therefore develop a joint channel estimation and prediction method for systems operating in V2X communication networks.

The purpose of using enhanced pilot patterns is to choose the most appropriate pilot pattern for tracking the dynamics of the channels better. We therefore have following remarks.

1) For low-mobility scenarios, pattern set 0 is able to track the dynamics of channels in the time domain.
2) For high-mobility scenarios with significant Doppler spread, pattern set 1 can be used for CFR estimation or ICI cancelation. In this case, the number of pilot symbols within one OFDM symbol are two times larger than that of pattern set 1, where channel tracking would benefit from more presence of pilot symbols.

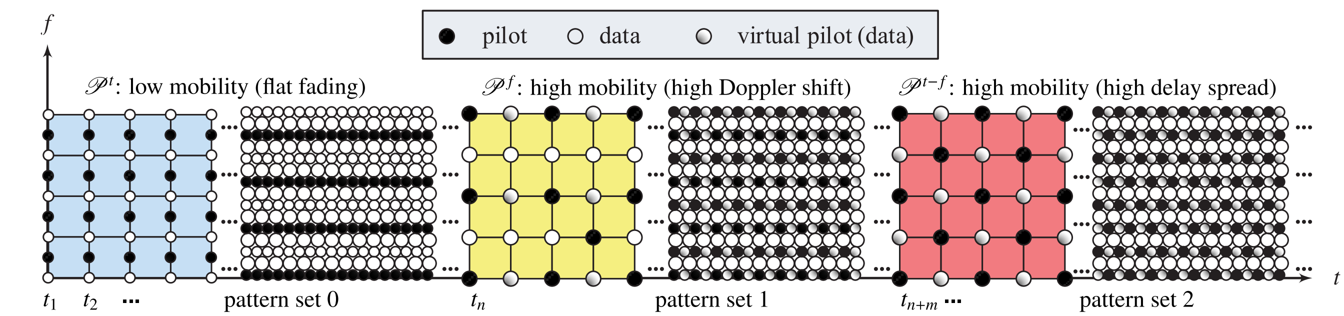

Fig. 2. Enhanced pilot patterns: pattern set 0 $\{\mathscr{P}_0(mT_s, \Delta, L_p)\}$ is a base mode for low mobility scenarios, whereas pattern set 1 $\{\mathscr{P}_0(2\times mT_s, \Delta/2, L_p - \Delta/2)\}$ and pattern set 2 $\{\mathscr{P}_0(mT_s, \Delta, L_p), \mathscr{P}_0(mT_s, \Delta, L_p - \Delta/2), \ldots\}$ is designed for a wide range of Doppler spread scenario and a high delay spread, respectively.

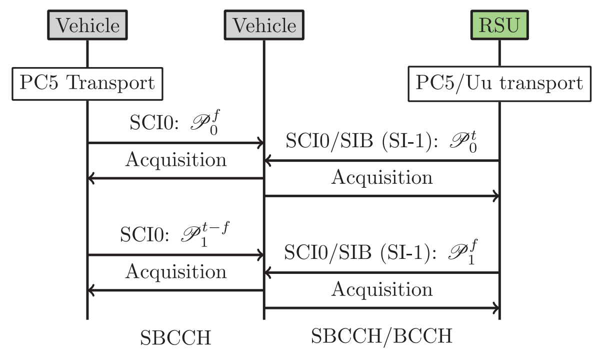

Fig. 3. Key exchange procedure to provide the pilot pattern via PC5 and/or Uu transport interfaces.

3) For high-mobility scenarios with high delay spread, pattern set 2 becomes more effective as the pilots hop from block to block, and allows a better detection on delay spread. In our pilot placement scheme, there are slight changes in the PHY layer, and a complete PHY layer implementation of the proposed scheme is feasible to be a SDR-based solution.

To support 5G V2X communications and autonomous vehicles applications, the Third Generation Partnership Project (3GPP) is now drafting the standard for 5G V2X, starting with Rel. 16 [4]. A new 3GPP study item on enhanced V2X model will particularly consider a direct D2D sidelink (PC5) and cellular link (Uu), where the D2D communication can be either unicast or broadcast without a closed-loop link control or feedback. In enhanced 5G V2X model, the radio environment should be considered in resource allocation, and user equipment should report the radio environment [1]. In this case, the resource allocation is changed based on the channel quality, accordingly, PC5 and Uu transport can be utilized to exchange pilot pattern.

To this end, we develop a protocol-specific mechanism, and Fig. 3 illustrates the procedure of exchanging pilot pattern directly among vehicles and between vehicle and RSU. The notification of updating pilot pattern can be carried by the sidelink broadcast control channel (SBCCH) and/or the traditional BCCH. The sidelink control information (SCI) messages are transmitted over physical sidelink control channels, and SBCCH provides system information to all vehicle terminals connected to the RSU. For simplicity, Fig. 3 only illustrates the signaling procedure in support of the information exchange of the pilot pattern. Details of this procedure are described in [33]. Additionally, one can see that direct V2V and V2I communications over the PC5 transport can satisfy stringent latency requirements, where the end-to-end latency can be reduced substantially. In the Uu transport mode, the pilot pattern can be carried by the system information block, which can be transmitted at a minimum interval (80 ms). Thus, the processing overhead is negligible when SCI0 and SI-1 transmission modes are available.

C. Optimal Pilot Placement for Channel Estimation

From (2) and (3), it is apparent that the channels can be estimated in a fairly simple way using the following supervised method.

For a given pilot placement, the channel estimation at pilot position can be obtained by achieving the minimal MSE

$$\underset{\hat{h}_p}{\operatorname{argmin}} \mathrm{MSE}_h = \frac{\{\left|h - \hat{h}_p\right|^2\}}{\{|h|^2\}} \tag{8}$$

where h is the best linear unbiased estimate for the channel coefficients and $\hat{h}_p$ is the estimated CIR at the pilot positions.

Let $h_v^{(i)}(n;\ k)$ be virtual pilot-aided channel estimates at the ith subcarrier of the kth OFDM symbol. As shown in Fig. 2, $h_v^{(i)}(n, k)$ can be predicted from the previous observations, which is given by $h^{(i)}(n;\ k) = [h_p^{(i)}(n;\ k-1), h_v^{(i)}(n; k-2), \ldots, h_v^{(i)}(n; k-\ell+1), h_p^{(i)}(n; k-\ell)]$. The channel prediction that is based on the ℓ previous CIRs that can be derived by [34]

$$\hat{h}_v^{(i)}(n;\ k+1) = \eta_k^{(i)} \oplus h^{(i)}(n;\ k) \tag{9}$$

where $\eta_k^{(i)}$ represents the prediction coefficients that are associated with the ith subcarrier on the kth OFDM symbol. Furthermore, the MMSE method can be utilized to predict the fading CIR and/or CFR from numerous past observations, so that the transmitted data can be recovered in this way.

Since the channel variation within two successive OFDM symbols could be viewed as linear, $h_v^{(i)}(n;\ k)$ can be refined in a fairly simple way by using iterative channel estimation, linear interpolator, and/or curve fitting algorithm [35], [36]. In a simplified way, the resulting update for $\hat{h}_v^{(i)}(n;\ k)$, i.e., the channel parameters and prediction coefficients of polynomial, can be calculated by using the Lagrange interpolation polynomial [37]. For a given set of data points (t_k, η_k), $k = 1, 2, \ldots, \ell$, the Lagrange basis function can be represented by

$$\xi_j(t) = \frac{\prod_{k=1,k\neq j}^{\ell}(t - t_k)}{\prod_{k=1,k\neq j}^{\ell}(t_j - t_k)} \tag{10}$$

where ξ_j is the channel coefficient at the jth time slot. Denote a general interpolation basis function by Ξ, the interpolating data points η_k can be obtained via appropriate basis function. As a consequence, the channel estimates can be updated using these virtual pilot symbols. Once all virtual pilot aided estimations are refined by (9), the next observation η_{k+1} for $h_v(n; k+1)$ can be refined on the basis of past measurements $\Xi\{\tilde{h}_v(n;\ k), h_p(n; k-1), \tilde{h}_v(n; k-2), \ldots\}$.

To reduce the number of channel coefficients required to be estimated and/or predicted, we use a basis expansion model (BEM) representation to approximate time-varying channels, where the variation of the channel is modeled by a basis expansion. Various traditional BEM designs have been reported to be capable of modeling the time variation of a channel, e.g., the complex exponential BEM, the polynomial BEM, and the discrete Karhuen–Loeve BEM [38]. The BEM coefficients are used to represent $h_l(n;\ k)$. The characteristics of channels can be expressed by a weighted sum of complex exponentials

$$h_l(n; k) = \sum_{q=-Q}^{Q} \bar{h}_l(q; k)\bar{b}_q(n; k) \tag{11}$$

where $\bar{h}_l(q; k)$ is the BEM coefficients for the lth tap of the kth OFDM symbol and $\bar{b}_q(n;\ k)$ represents the orthonormal basis functions. Owing to the maximal energy concentration in the main lobe, the discrete prolate spheroidal BEM (DPS-BEM) sequences can be used to parameterize a deterministic channel, allowing a generalized nonsymmetric (and even discontiguous) band limit in the time and frequency domains. For generalized DPS channels, the DPS-BEM is constructed with a special vector of the autocorrelation R, which is associated with a rectangular Doppler spectrum and used to indicate the maximum time variation of a wireless communication channel. For the estimation of channels that are modeled by a BEM, we only need to estimate the BEM coefficients [39]. As the details of the modeling process are out of the scope of this paper, we do not present the details here without losing completeness, and interesting readers can refer to [38], [40], and [41].

In a similar manner, the CFR H_v at particular subcarriers and the virtual pilot position can be obtained, which allows improving the accuracy of the CFR prediction value $\tilde{H}_v$ by using the method discussed above. The CFR H_v and the BEM coefficients $\bar{b}_q(n;\ k)$ of the taps can be jointly estimated based on the received OFDM symbol block. From (10), the channel gains $H^{(j)}(n;\ k)$ and ICI terms $\mathrm{ICI}^{(j)}$ can be obtained, including the statistical property of the ICI. With the aid of accurate channel estimation, ICI could be reconstructed and removed from the received signal.

IV. Solution to MDP-Based Pilot Optimization

In this section, we derive analytical expressions of mutual information between the transmitter and receiver so as to jointly evaluate the effects of channel variation in time and frequency domains. With mutual information, the degradation of OFDM systems can be quantified under different channel conditions. Taking the mutual information as the system performance metric, the most significant characteristics of time-varying channel can be separated and the objective of the optimal pilot placement is to maximize the mutual information, i.e., system capacity. Finally, the MDP-based pilot optimization policy is shown to be solved by value iterations at the end of this section.

A. Evaluation Criteria Based on Mutual Information

From the signal model constructed in (1) and (2), one can see that two input–output pairs x, y and X, Y are expressed in time and frequency domain, respectively. The mutual information $I(x; y)$ and $I(X; Y)$ can be defined as

$$I(x; y) = \mathcal{H}(x) - \mathcal{H}(x|y) \tag{12a}$$

$$I(X; Y) = \mathcal{H}(X) - \mathcal{H}(X|Y) \tag{12b}$$

where $\mathcal{H}(\cdot)$ denotes entropy. Similarly, let $x = \{x^1, x^2, \ldots, x^i\}$ and $X = \{X^1, X^2, \ldots, X^i\}$ be the sequence input, and accordingly $y = \{y^1, y^2, \ldots, y^j\}$ and $Y = \{Y^1, Y^2, \ldots, Y^j\}$ be the sequence output. The average mutual information of $I(x; y)$ and $I(X; Y)$ per sample can be calculated in terms of their probabilistic density functions $p(x)$, $p(y)$, and $p(X)$, $p(Y)$ by

$$I\left(x^i; y^j\right) = \sum_i \sum_j p\left(x^i, y^j\right)\log_2\left(\frac{p\left(x^i, y^j\right)}{p\left(x^i\right)p\left(y^j\right)}\right) \tag{13a}$$

$$I\left(X^i; Y^j\right) = \sum_i \sum_j p\left(X^i, Y^j\right)\log_2\left(\frac{p\left(X^i, Y^j\right)}{p\left(X^i\right)p\left(Y^j\right)}\right) \tag{13b}$$

where $p(\cdot)$ is used to describe the *posterior* distribution in time and frequency domains. Mutual information has been verified as an efficiency metric for performance assessment and is equivalent to the traditional estimation metrics (e.g., least square and MMSE) [42].

Consequently, mutual information measurement is more convenient for predefined channel variant collection χ and ψ. The dynamics of the channels are represented by mutual information and can be treated as a multivariate variable. Considering the effects of channel parameters ϕ and Φ in time and frequency domains, we can calculate the gradient of mutual information, which can be easily derived from [43]

$$\frac{\partial}{\partial\phi}I(x|y) = \mathbb{E}\left\{\frac{\partial \log_2 P_{y|x}^{\phi}}{\partial\phi}\log_2 P_{x|y}^{\phi}\right\},\ \ \phi \in \chi \tag{14a}$$

$$\frac{\partial}{\partial\Phi}I(X|Y) = \mathbb{E}\left\{\frac{\partial \log_2 P_{Y|X}^{\Phi}}{\partial\Phi}\log_2 P_{X|Y}^{\Phi}\right\},\ \ \Phi \in \psi. \tag{14b}$$

Observing (14a) and (14b), we can find a distribution to maximize $I(X;\ Y)$ and $I(x;\ y)$. For every input distribution $P_{y|x}^{\phi}$ and $P_{y|x}^{\phi}$, the optimal $\mathscr{P}^*$ can be numerically determined by maximizing the mutual information with binary inputs. By substituting them into the corresponding terms in (7), we have

$$\arg\max_{\phi\in\chi} \; I(x;y,\pi)\big|_{\phi} \;\text{ or }\; \arg\max_{\Phi\in\psi} \; I(X;Y,\pi)|_{\Phi}$$
$$\text{s.t. } \; \pi = \{\mathscr{P}_0^*, \mathscr{P}_1^*, \ldots, \mathscr{P}_j^*\} \;\; \forall\, \mathcal{S} \tag{15}$$

where $\mathscr{P}_j^*$ denotes all possible pilot placements in state space $\mathcal{S}$. In the next section, we will develop a control policy to obtain $\mathscr{P}^*$.

B. Determining Optimal Pilot Placement Policy

In our case, the MDP-based pilot optimization is defined as the tuple $(\mathcal{M}) = (\mathcal{T}, \mathcal{S}, \mathcal{A}, \mathcal{P}(s, a, s'), \mathcal{R}(s, a))$, and we primarily deal with discrete sets of states and actions. Given a finite horizon, the objective of an MDP is to find an optimal policy $\pi^* : \mathcal{S} \to \mathcal{A}$, which maximizes the expected reward $\mathcal{R}(s, a)$. We define the five elements of MDP to facilitate implementation of the pilot optimization-based policy.

1) *Finite Decision Epochs:* $\mathcal{T} = \{1, 2, \ldots, N\}$ corresponds to a statistical period of the packet. In this paper, we assume that the length of the data packet consists of 256 OFDM symbols, resulted from fixed decision epochs.
2) *States and Actions:* We denote $\mathcal{Q}_\pi(s, a : s \in \mathcal{S}, a \in \mathcal{A})$ as the set of state-action pairs for a given policy. All possible channel states $a \in \mathcal{S}$ can be observed at each epoch. In a state $s \in \mathcal{S}$, the decision maker selects an action $a \in \mathcal{A}$, where action a is chosen according to a pilot placement policy π.
3) *Rewards and Transition Probabilities:* For current channel state, the optimal pilot placement policy π indicates that the best action a is chosen to maximize reward $\mathcal{R}$. The transition probabilities represent that state s_i moves to state $s_j \in \mathcal{S}$ with conditional probability $p^{(t)}(s_j|s_i; a)$ at time slot t.
4) *Decision Policy:* For the finite horizon problem, a policy π is a sequence of decision rules $\mathcal{D} = \{d_1(a_i), d_2(a_j), \ldots\}, d_i \in D_i, i \in \mathcal{T}$, which can be viewed as a function mapping from the state space to action.
5) *Measurement Criteria:* The optimal policy π^* is to maximize the system capacity $\mathcal{C}(\mathscr{P}^*)$ with respect to preset mutual information measurement criteria.

Corresponding to an action a, the state transition could be understood as a random event, and the probability from current state to $s^{(t+1)}$ depends on the current channel state $s^{(t)}$. Considering K successive OFDM time slots, by the fundamental property of an Markov chain, the probability of the next state can be generally computed by [30]

$$\mathcal{P}\left(s^{(t)}, \ldots, s^{(t+K)}\right) = \prod_{k=0}^{K-1} \mathcal{P}\left(s^{(t+k)} \middle| s^{(t+k-1)}\right). \tag{16}$$

In reality, the accurate state transition probability is difficult to obtain. Fortunately, the study in [27] proved that the state transition probability depends on the total transition rate, and an analytical expression of the state transition probability was given. Accordingly, we propose an approximate method to compute one step state transition probability $\mathcal{P}_a(s, s')$. Using the mathematical structure in (14a) and (14b), the channel changes state in the form of the gradient of mutual information, which is equivalent to transient transition rate, e.g., a gradient descent means capacity loss. It lies in the fact that the state transition can be quantified in terms of the gradient of mutual information accumulated during every decision epoch. Define $\mathcal{G}_\phi(s^{(t)}|s^{(t-1)})$ to be the state transition rate (normalized with min–max method) corresponding to the gradient of mutual information between transient states. Then, the estimated $\hat{\mathcal{P}}_a(s, s')$ accumulated over a specified interval of time can be represented as

$$\hat{\mathcal{P}}_a(s, s') = \prod_{k=0}^{K-1} \Pr.\left[1 + \mathcal{G}_\phi\left(s^{(t+k)} \middle| s^{(t+k-1)}\right)\right]. \tag{17}$$

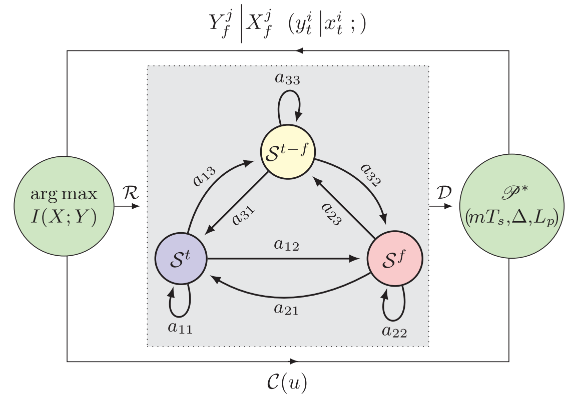

Fig. 4. From input $I(X; Y)$ to an MDP and output $\mathscr{P}^*$: a controlled Markov chain based on a action transit matrix, e.g., a_{12}.

In Section III-B, we proposed an enhanced pilot pattern scheme, and showed that a small number of pilot placements are feasible to estimate time-varying channels. This suggests that the subspace method could be applied to identify the most significant characteristic of a channel. Therefore, the state space can be further reconstructed in a similar way as $\mathcal{S} = \{\mathcal{S}^t, \mathcal{S}^f, \mathcal{S}^{t-f}\}$, where $\mathcal{S}^t$, $\mathcal{S}^f$, and $\mathcal{S}^{t-f}$ are the subsets of $\mathcal{S}$, which represent the three typical intensities of channels variations [20]. With the subspace method, we can map $\mathcal{S}^t, \mathcal{S}^f, \mathcal{S}^{t-f}$ to specific $\mathscr{P}^t$, $\mathscr{P}^f$, $\mathscr{P}^{t-f}$, respectively. It will significantly reduce the number of state-space pairs and obtain the solution by value iterations using linear programming, so that the action sets for optimal control policy in (17) can be further shrunken. In this paper, the time-varying channel is modeled as a finite-state Markov channel (FSMC), and its conditional input/output probability of FSMC can be determined by the channel state at time n [44]. In (14a) and (14b), the channel mutual information has been formulated by a closed-form continuous function of the input distribution, and the gradient of mutual information can be thereby utilized to determine the state transition.

To illustrate the state transition of an MDP, Fig. 4 illustrates a simplified signal-flow chart, where the action to be taken at each decision epoch is either to activate a new pilot pattern, to deactivate a currently active pilot pattern, or to stay the same.

As depicted in Fig. 4, the average mutual information is calculated from the input–output pairs $(x^i; y^i)$ and $(X^j; Y^j)$.

For the current observed state $\mathcal{S}^t$, we carry out an action randomly chosen from a probability distribution over $\mathcal{A}(y^i|\hat{h}_p)$. Simultaneously, χ and ψ, as well as the effect of channel variation in time and frequency-domain can be identified. At the beginning, we assign a fixed pilot pattern to s_i ($s_i \in \mathcal{S}$) in the absence of any measurement information. If the current channel state satisfies the maximum capacity bound of $I_{\max}$ during an observation epoch, it will be maintained. In the next decision-making epoch, once the transition to the next state has occurred, a new action $a_k \in \mathcal{A}$ should be chosen, and the process should be repeated iteratively. Additionally, the symbol rate is much faster than the fading rate, and thereby a higher convergence rate is achieved.

Using the finite MDP above, the optimal policy can be solved by conventional value iteration algorithms. Define $\mathcal{V}_\pi(\mathcal{S}_i)$ as the minimum expected cost to reach a goal from s. To determine the optimal pilot placement policy with the value iteration algorithm, four essential steps are required.

Step 1: Define $\mathcal{V}_\pi(s_i)$ as the minimum expected cost to obtain the optimal $\mathscr{P}^*$ from s. Then, set the start state $s_0 \in S^t$ and initialize $\mathcal{V}_0$ arbitrarily. For each s, the value iteration can be calculated by

$$\mathcal{V}_\pi(\mathcal{S}_i) = \mathcal{R}(\mathcal{S}_i) + \gamma \sum_{\mathcal{S}_i'} \mathcal{P}(\mathcal{S}_i|\mathcal{S}_i, a = \pi(\mathcal{S}_i))\mathcal{V}_\pi\left(\mathcal{S}_i'\right) \tag{18}$$

where $\gamma \in (0, 1]$ is the discount factor.

Step 2: According to the Bellman equation [30], the optimal value function $\mathcal{V}^*$ is the minimum expected cost to reach a goal from this state, and can be updated iteratively by

$$\mathcal{V}^*(\mathcal{S}_i) = \max_{a\in\mathcal{A}}\left\{\mathcal{R}(\mathcal{S}_i, a) + \gamma \sum_{\mathcal{S}_i'} \mathcal{P}\left(\mathcal{S}_i'|\mathcal{S}_i, a = \pi(\mathcal{S}_i)\right)\mathcal{V}_\pi^*\left(\mathcal{S}_i'\right)\right\} \tag{19}$$

where $\mathcal{V}_\pi^*(\mathcal{S})$, $s \in \mathcal{S}_i$, is unique. Generally, a linear programming algorithm continues until the value of $\mathcal{V}^*(\mathcal{S}_i)$ is determined [30].

Step 3: Given a minimized error bound ϵ, if $|\mathcal{V}^{n+1} - \mathcal{V}^n| < \epsilon$, then move to the next step, otherwise go back to step 2.

Step 4: The optimal policy π^* for state transition can be written as

$$\pi^*(a) = \arg\max_{a\in\mathcal{A}}\left\{\mathcal{R}(\mathcal{S}_i, a) + \gamma \sum_{\mathcal{S}_i'} \mathcal{P}\left(\mathcal{S}_i'|\mathcal{S}_i, a = \pi(\mathcal{S}_i)\right)\mathcal{V}_\pi^*\left(\mathcal{S}_i'\right)\right\}. \tag{20}$$

Finally, according to (8), the output $\mathscr{P}^*$ based on MMSE estimation is used to yield optimal channel estimates.

The optimal pilot pattern selection, acquisition and notification are conducted in an online manner, as outlined in Algorithm 1. Note that, optimal action determination based on MDP is to find an optimal action for each specific state that maximizes the cumulative function of expected rewards $\mathcal{R}$. After convergence, the optimal decision of pilot pattern selection can be made at decision epochs $\mathcal{T}$, and the updating pilot pattern can be transported via PC5 and/or Uu transport interfaces.

TABLE I
DELAY PROFILES OF MULTIPATH FADING CHANNEL MODELS

Mobility	Low	High	High
Channel model	EPA	EVA	ETU
Number of channel taps	7	9	9
Tap delay $\tau_{\max}$ (ns)	30	710	1600
Relative power (dB)	-2.0	-9.1	-3.0
$f_{D\max}$ (Hz)	37.5	300	150

Algorithm 1 Online Optimal Pilot Pattern Selection, Acquisition, and Notification

Input: $mT_s,\ \Delta,\ L_p;\ \mathbf{x}(n;\ k)$
Ouput: $\mathscr{P}^*$

procedure OPTIMAL PILOT SELECTION
initialization: $\mathscr{P}_0 \in \mathscr{P}^t,\ \mathcal{S} \in \mathcal{S}^t$ ▷ flat fading
  repeat
   Estimate $h(\tau;t)$, $\mathbf{H}(\tau;f)$
    for all $\mathcal{S}$ **do** ▷ complexity reduction Evaluate $\mathcal{S}$: $I(x|y)$, $I(X|Y)$
     if $\mathcal{S} \in \mathcal{S}^f$ **then**
      $\mathscr{P} \in \mathscr{P}^f$ ▷ high Doppler shift
     else if $\mathcal{S} \in \mathcal{S}^{t-f}$ **then**
      $\mathscr{P} \in \mathscr{P}^{t-f}$ ▷ high delay spread
     else
      $\mathscr{P} \in \mathscr{P}^t$ ▷ flat fading
     end if
    end for
Make decision: $\mathcal{M}(\mathcal{T}, \mathcal{S}, \mathcal{A}, \mathcal{P}, \mathcal{R})$
  until $\arg\max \sum_{t=0}^{\infty} \mathcal{R}_{a_t}(s_t, s_{t+1})$ ▷ rewards
Make action: $a \to \mathscr{P}^*$
Transport $\mathscr{P}^*$: PC5 $\longleftrightarrow$ PC5/Uu
end procedure

V. NUMERICAL RESULTS

A. Simulation Settings

This section considers the deployment scenarios of 5G V2I system in the highway for urban connected cars. To carry out simulations to verify the analysis presented in this paper, we first need to specify the simulation parameters. A typical set of parameters of the PHY layer used in simulations is listed as follows. Here, we stipulate an OFDM system with the number of FFT points $N = 64$, operating in a 20 MHz channel with a frequency separation $\Delta_f = 1/T_s = 0.3125$ MHz, such that the symbol period $T_s = 3.2$ μs. The length of cyclic prefix is set to 4 μs. In total, 52 subcarriers are employed in the OFDM system, of which 48 subcarriers are used for data transmission, and the 4 remaining are used as pilots. In Section III-B, we have designed an enhanced pilot pattern scheme to deal with three typical vehicular communication scenarios. Table I summarizes the delay profiles of a multipath fading channel. We adopt the extended pedestrian A model (EPA), extended vehicular A model (EVA) and extended typical urban model (ETU) to describe above typical vehicular communication scenarios [45]. The channel is approximated by a BEM representation, while the four-ray model is used and

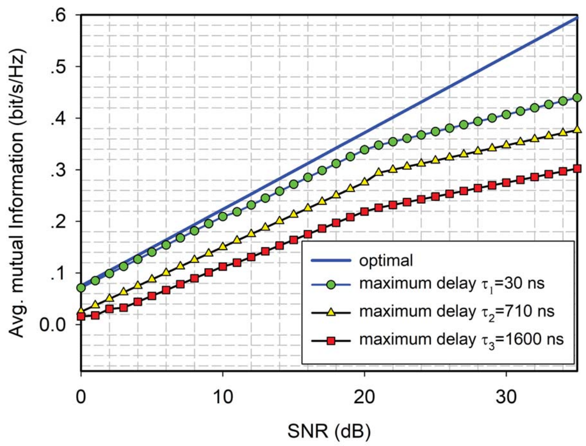

Fig. 5. Average mutual information versus SNR (time domain): $I(x; y)$ were obtained from 1000 OFDM symbols. α is set to be 0.95.

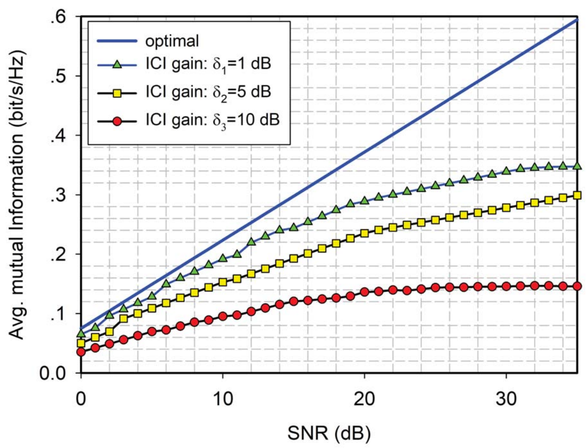

Fig. 6. Average mutual information versus SNR (frequency domain): $I(X; Y)$ is obtained from 1000 OFDM symbols. α is set to be 0.95.

each ray is generated independently according to the variations of the BEM coefficients across OFDM blocks.

We consider three typical vehicle scenarios, highway (120 km/h), urban (60 km/h), and congested road (15 km/h). In this paper, the maximum carrier frequency over all frequency bands is $f_c = 2690$ MHz and the corresponding maximum Doppler frequency at velocity $v = 120$ km/h is $f_{D_{\max}} = 300$ Hz. With the maximum tap delay $\tau_{\max}$ and maximum Doppler frequency ($f_{D_{\max}}$), the power delay profile $[0, \tau_{\max}]$ and maximum Doppler power spectral density $[f_{D_{\max}}, f_{D_{\max}}]$ are used to parameterize generalized DPS sequences in time and frequency domains, respectively. To investigate the impact of V2X in high Doppler shifts, we mainly simulate a V2V scenario operating over a doubly selective channel that is modeled by BEM parameters [38]. Finally, the performance of channel estimator, BER performance and mutual information are investigated using Monte Carlo simulations.

B. Discussion of Numerical Results

Figs. 5 and 6 illustrate the measurement performance of the average mutual information criteria in the time and frequency domains. One can observe that ICI can be efficiently evaluated by the mutual information criteria, and shows a high resolution of measurement on time delay and frequency offset. We selected the RMS delay spread of a TU6 channel $\tau_{\text{rms}} = 1.1\ \mu$s to reveal the characteristic of channel in the time domain, while setting the delay between two channels as $\tau_1 = 30$ ns, $\tau_2 = 710$ ns, $\tau_3 = 1600$ ns. Fig. 5 shows that with the increase of signal-to-noise ratio (SNR), the resolution increases. Fig. 6 shows that the evaluation of the channel variation in the frequency domain. According to (3), we only consider the additive ICI components. Another observation from Fig. 6 is that there is no significant improvement of capacity in high speed scenarios, where the ICI gain is set to be $\delta_1 = 1$ dB (15 km/h), $\delta_2 = 5$ dB (60 km/h) and $\delta_3 = 10$ dB (120 km/h). To accelerate the value iteration process, we adopt $\gamma = 0.985$ for the discount factor with $\varepsilon = 0.015$ for convergence. We subsequently observe that the optimal iteration algorithm will converge to the optimal value within 500 iterations.

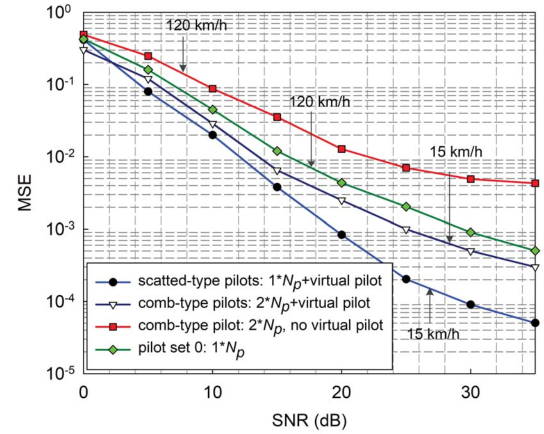

Fig. 7. Channel estimator performance in high-mobility scenario: MSE versus SNR, given OFDM block length $N = 2000$, $N_P = 4$.

Fig. 7 shows that with enhanced pilot patterns (refers to Fig. 2), the performance of MMSE channel estimator can be significantly improved in a fast time-varying channel. When a linear fitting method is adopted to obtain the predicted CIR at the virtual pilot position, we observe that the use of virtual pilots can lead to significant performance gains. Fig. 7 also investigates into two different high mobility scenarios, in which channels vary in the time and frequency domains. From this figure, one can see that the MSE is very low, which ensures the robustness of the channel estimator. Fig. 8 further illustrates the BER curves of different pilot optimization schemes associated with the specified decisions. We looked into the channel state matched pilot arrangement scheme to compare with the fixed pilot design, which neglects the physical properties of the current channel. In all cases, the channel state matched pilot patterns outperform the fixed pilot pattern. It indicates that the proposed scheme can provide better BER performance. We also observe that there are very small performance differences among the channel state matched pilot placements, which confirm the generality of the proposed method.

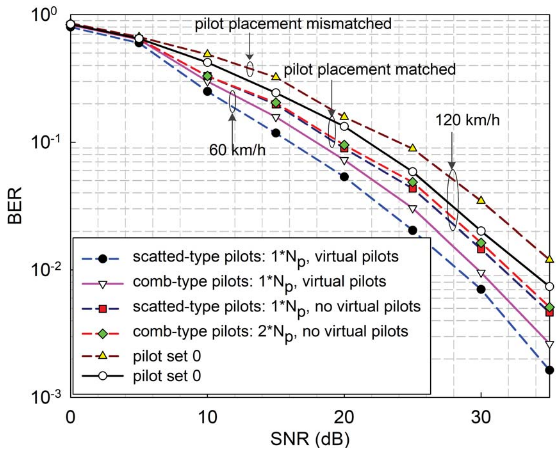

Fig. 8. BER performance for QPSK modulation and 1/2 coding rate, given OFDM block length $N = 2000$, $N_P = 4$.

Finally, we further investigate the performance of channel estimation with different decision-based solutions, namely the optimal policy, near-optimal policy, fixed policy, and random policy. As mentioned earlier in Section IV-B, the optimal policy is obtained by Bellman's equation based on the MDP model, and the subspace method is used to reduce the number of state-space pairs for fast convergence of value iteration. In this simulation study, the near-optimal policy is also based on the MDP model without the subspace restraint. The random policy is that the MDP agent is not activated and the pilot patterns are randomly solved by the exhaustive search algorithm [46]. Fixed policies are traditional pilot placement based on the state-of-the-art techniques in [12], [17], [21], [26], and [39], where the equispaced and equipowered pilot sequences are prevalent in the case of high mobility scenarios. Typically, these schemes with respect to the MSE channel estimator used block-type and/or comb-type pilot tones placed on uniformly interleaved groups to yield a set of fixed pilot patterns, including an optimal training design. In the subsequent simulation, we apply the design of pilot tones in [26] to be the simulation case of fixed pilot policy, which is mapped to pilot pattern 0 ($N_p = 4$) in a simple manner. For the purpose of comparison, we insert the same proportion pilots according to the method stated in [26] for a straightforward implementation following our pilot scheme. In a practical vehicular communication environment, the closed forms for the dynamics of channel, e.g., the state transition probabilities, are generally difficult to obtain. However, the statistical channel characteristics make it possible to reflect the realistic behavior of channel and the state transition probability can be derived as the product of mutual information (see Section IV-A). To achieve the numerically solvable state transition probability for effective and viable simulations, we investigate the estimation of channels by using a Gauss Markov process to simulate the channel dynamics. The correlation coefficient α (within one decision epoch) is further utilized to obtain desirable channel fading conditions that range from severe to moderate.

By using the calculation method in (19), the value iteration algorithm is used to select the optimal pilot pattern for the dynamics of the vehicular channels. The average iteration number of the decision at all state transitions (i.e., channel realizations) are illustrated in Table II. We investigate the expected value iterations of all channel realizations, e.g., the artificially generated vehicular channel happens to start from EPA to EVA, from EPA to ETU and so on. The result shows that the average iteration number of the decision from the optimal policy have consistently fewer iterations than the approximate optimal policy. In this paper, the objective value function is updated online for multiple state-action pairs at each time-slot. Once the transition probabilities and rewards are calculated, the decision-maker takes an action and evaluates the corresponding rewards and state transition. Admittedly, if the prior knowledge of channel statistics can be incorporated in advance, an offline iteration approach will significantly reduce the number of iterations required for convergence. In the case of vehicular channels, however, since the channel statistics can only be obtained from the received signals, the offline method may be impractical for dealing with the fast time-varying vehicular communication scenarios. Fig. 9 further illustrates the convergence property of the proposed optimal and approximate optimal policy, while the state transitions of vehicular channel are preset to start from EPA to EVA, and to ETU. It generally shows that the optimal policy could provide a faster convergence rate than the approximate optimal policy, and after 500 iterations, the values are close to the final converged results. It is worth noting that although the online value iteration has many iterations, it is possible to gather sufficient data to accurately estimate the one step state transition probability $\mathcal{P}_a(s, s')$ (refer to Section IV-B). Moreover, excessive update of the pilot pattern may lead to capacity loss due to feedback overhead. Therefore, large number of decision actions for pilot selection are not necessary, and the convergence of the value iteration is still within an acceptable range.

TABLE II
RESULTS OF VALUE ITERATION ALGORITHM FOR DECISION-MAKER

Channels	Average iteration number	
	Optimal	Approximate optimal
EPA → EVA	230	700
EPA → ETU	380	660
EVA → ETU	240	710
EVA → EPA	220	730
ETU → EPA	200	640
ETU → EVA	350	680

The results illustrated in Figs. 10 and 11 demonstrate the MMSE performance of channel estimator versus the fading correlation coefficient α in the high SNR regime (20 dB). The range of α has been varied from 0.85 to 0.99, in which a smaller α means that the channel varies faster. For comparison, we take the virtual pilot-assisted case as shown in Fig. 2 as a benchmark, and adopt $\gamma = 0.95$ for the discount factor with $\varepsilon = 0.02$ for convergence. Fig. 10 depicts the MMSE performance of the CIR estimations, with a severe channel variation in the time domain. It is obvious that the optimal policy performs better, whereas the random policy

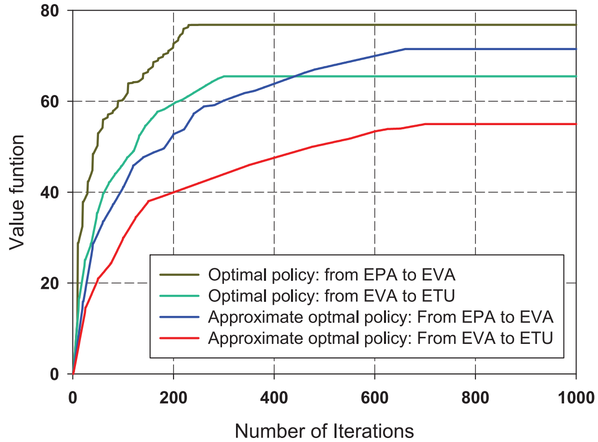

Fig. 9. Convergence property of value iteration with a statistical average of 50 trials.

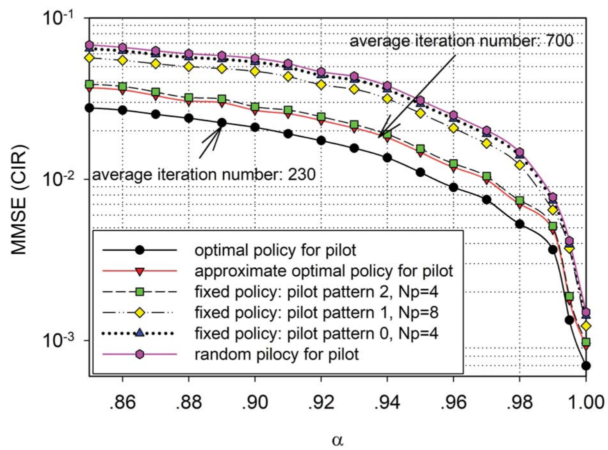

Fig. 10. MMSE performance (CIR estimation) for QPSK modulation and 1/2 coding rate, given OFDM block length $N = 2000$, $N_P = 4$, and SNR = 20 dB.

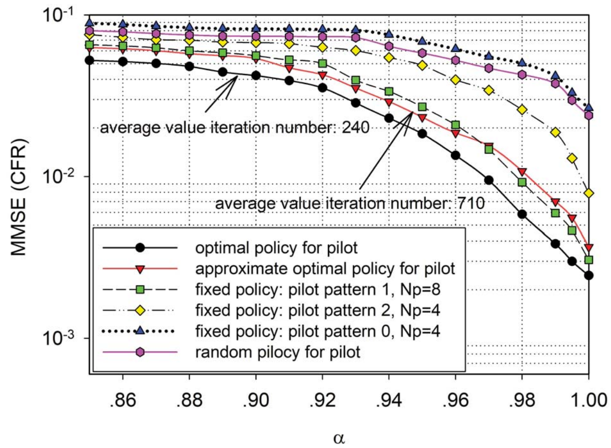

Fig. 11. MMSE performance (CFR estimation) for QPSK modulation and 1/2 coding rate, given OFDM block length $N = 2000$, $N_P = 4$, and SNR = 20 dB.

performs the worst. We investigate the convergence property of value iteration with a statistical average of 50 trials, and observe that the optimal policy with subspace restraint has better convergence than that of the near-optimal policy. The convergence rate of value iteration for optimal policy is generally faster when compared to the approximate optimal policy. This is because the subspace restraint reduces the dimension of the control action space involved. We also observe that the optimal policy solution can be determined in each decision epoch, which is well suited for the online value iteration algorithm. Compared to the state-of-the art [26] with regard to a fixed pilot policy, it can be seen that enhanced pilot pattern 1 and pattern 2 lead to a smaller MMSE of channel estimation when the channels vary in time and frequency domains. As expected, with the increase of pilot numbers, the channel estimator provides better performance, and with the constant channel condition ($\alpha > 0.99$), all pilot patterns exhibit nearly the same performance.

Fig. 11 illustrates the comparison of the MMSE performance of the CFR estimation, with a severe channel variation in the frequency domain. The parameter setting in Fig. 11 is the same as in Fig. 10 and a similar analysis is performed in the frequency domain. As expected, the system using an optimal policy of pilot placement gives the minimum channel estimation MSE, and can lead to significant performance gains. From Fig. 11, it can be observed that the performance of channel estimation strongly depends on the number of pilot symbols. As can be seen from Fig. 11, we can also achieve the optimal policy within each decision epoch, thus, an online value iteration algorithm is applicable. For the fixed policy, our results suggest that more pilot symbols (patterns 1 and 2) are allocated, the better the estimation and the tracking performance will be and $Np = 8$ is sufficient to achieve good performance under the given high-mobility conditions (i.e., a small α). In addition, another important finding from Figs. 10 and 11 is that, for a small α (less than 0.9), it is hard to satisfy the performance of the estimator even if more pilot symbols are in use. According to the simulation, the error floor emerges at a relatively high SNR regime and the enhanced pilot patterns are not effective anymore. This also suggests that the impact of Doppler shift is more harmful than the time delay spread with the same extent, which is common for time-varying channels. Moreover, from the consequences of Figs. 10 and 11, the optimal policy and near-optimal policy solutions will enhance the channel estimation especially for channels with a high Doppler spread. It may imply that the optimal policy and near-optimal policy would be optimistic results for fast time-varying channels, whereas the random pilot placement policy is ineffective to deal these situations.

VI. Conclusion

In this paper, a low-complexity pilot placement optimization method based on a finite MDP was proposed to achieve high transmission performance for 5G V2X systems adopting pilot-assisted OFDM technology. We have derived expressions of mutual information to evaluate the effects of the channel variation in time and frequency domains. The use of enhanced pilot patterns provides a significant complexity reduction for solving the formulated optimization problem. Simulation results confirmed that the proposed method is effective to track fast time-varying vehicular channels. Moreover, the proposed estimation schemes and algorithms in this paper can also be easily extended to other OFDM systems with a slight modification.

ACKNOWLEDGMENT

The authors would like to thank the anonymous reviewers for their insightful comments that significantly improved the quality of this paper.

REFERENCES

[1] A. Kousaridas, D. Medina, S. Ayaz, and C. Zhou, "Recent advances in 3GPP networks for vehicular communications," in *Proc. IEEE Conf. Stand. Commun. Netw. (CSCN)*, Helsinki, Finland, Sep. 2017, pp. 91–97.

[2] M. Boban, K. Manolakis, M. Ibrahim, S. Bazzi, and W. Xu, "Design aspects for 5G V2X physical layer," in *Proc. IEEE Conf. Stand. Commun. Netw. (CSCN)*, Berlin, Germany, Oct./Nov. 2016, pp. 1–7.

[3] E. Vlachos, A. S. Lalos, K. Berberidis, and C. Tselios, "Autonomous driving in 5G: Mitigating interference in OFDM-based vehicular communications," in *Proc. IEEE 22nd Int. Workshop Comput.-Aided Model. Design Commun. Links Netw. (CAMAD)*, Lund, Sweden, Jun. 2017, pp. 1–6.

[4] 5G-PPP Automotive Working Group. (2018). *A Study on 5G V2X Deployment*. [Online]. Available: https://5g-ppp.eu/wp-content/uploads/2018/02/5G-PPP-Automotive-WG-White-Paper_Feb.2018.pdf

[5] G. Araniti, C. Campolo, M. Condoluci, A. Iera, and A. Molinaro, "LTE for vehicular networking: A survey," *IEEE Commun. Mag.*, vol. 51, no. 5, pp. 148–157, May 2013.

[6] J. Contreras, S. Zeadally, and J. A. Guerrero-Ibanez, "Internet of Vehicles: Architecture, protocols, and security," *IEEE Internet Things J.*, to be published, doi: 10.1109/JIOT.2017.2690902.

[7] K. J. Ahmed and M. J. Lee, "Secure, LTE-based V2X service," *IEEE Internet Things J.*, to be published, doi: 10.1109/JIOT.2017.2697949.

[8] N. Ksairi, B. Tomasi, and S. Tomasin, "Pilot pattern adaptation for 5G MU-MIMO wireless communications," in *Proc. IEEE 17th Int. Workshop Signal Process. Adv. Wireless Commun. (SPAWC)*, Edinburgh, U.K., Jul. 2016, pp. 1–6.

[9] L. Tong, B. M. Sadler, and M. Dong, "Pilot-assisted wireless transmissions: General model, design criteria, and signal processing," *IEEE Signal Process. Mag.*, vol. 21, no. 6, pp. 12–25, Nov. 2004.

[10] C. F. Mecklenbrauker *et al.*, "Vehicular channel characterization and its implications for wireless system design and performance," *Proc. IEEE*, vol. 99, no. 7, pp. 1189–1212, Jul. 2011.

[11] *Overview of OTFS Waveform for Next Generation RAT*, 3GPP Standard R1-162929, Apr. 2016.

[12] X. Ma, M.-K. Oh, G. B. Giannakis, and D.-J. Park, "Hopping pilots for estimation of frequency-offset and multiantenna channels in MIMO-OFDM," *IEEE Trans. Commun.*, vol. 53, no. 1, pp. 162–172, Jan. 2005.

[13] X. Cai and G. B. Giannakis, "Error probability minimizing pilots for OFDM with M-PSK modulation over Rayleigh-fading channels," *IEEE Trans. Veh. Technol.*, vol. 53, no. 1, pp. 146–155, Jan. 2004.

[14] T. Cui and C. Tellambura, "Joint frequency offset and channel estimation for OFDM systems using pilot symbols and virtual carriers," *IEEE Trans. Wireless Commun.*, vol. 6, no. 4, pp. 1193–1202, Apr. 2007.

[15] I. Budiarjo *et al.*, "On the use of virtual pilots with decision directed method in OFDM based cognitive radio channel estimation using 2x1-D Wiener filter," in *Proc. IEEE ICC*, Beijing, China, May 2008, pp. 703–707.

[16] J.-S. Baek and J.-S. Seo, "Efficient pilot patterns and channel estimations for MIMO-OFDM systems," *IEEE Trans. Broadcast.*, vol. 58, no. 4, pp. 648–653, Dec. 2012.

[17] I. Barhumi, G. Leus, and M. Moonen, "Optimal training design for MIMO OFDM systems in mobile wireless channels," *IEEE Trans. Signal Process.*, vol. 51, no. 6, pp. 1615–1624, Jun. 2003.

[18] M. Dong, L. Tong, and B. M. Sadler, "Optimal insertion of pilot symbols for transmissions over time-varying flat fading channels," *IEEE Trans. Signal Process.*, vol. 52, no. 5, pp. 1403–1418, May 2004.

[19] P. Banelli, R. C. Cannizzaro, and L. Rugini, "Data-aided Kalman tracking for channel estimation in doppler-affected OFDM systems," in *Proc. IEEE ICASSP*, Honolulu, HI, USA, Apr. 2007, pp. 133–136.

[20] L. Ljung, *System Identification: Theory for the User*, 2nd ed. Englewood Cliffs, NJ, USA: Prentice-Hall, 1999.

[21] M. Karami, A. Olfat, and N. C. Beaulieu, "Pilot symbol parameter optimization based on imperfect channel state prediction for OFDM systems," *IEEE Trans. Commun.*, vol. 61, no. 6, pp. 2557–2567, Jun. 2014.

[22] M. Karami and N. C. Beaulieu, "Channel adaptive power allocation and pilot optimization for OFDM systems," in *Proc. IEEE Glob. Commun.*, Sydney, NSW, Australia, Dec. 2012, pp. 4893–4898.

[23] E. Y. Menta, K. Ruttik, and R. Jäntti, "Dynamic pilot scheduling scheme for 5G outdoor ultra-dense network," in *Proc. IEEE Conf. Stand. Commun. Netw. (CSCN)*, Helsinki, Finland, Sep. 2017, pp. 281–286.

[24] W.-C. Chen and C.-D. Chung, "Spectrally efficient OFDM pilot waveform for channel estimation," *IEEE Trans. Commun.*, vol. 65, no. 1, pp. 387–402, Jan. 2017.

[25] Z. Sheng, H. D. Tuan, H. H. Nguyen, and Y. Fang, "Pilot optimization for estimation of high-mobility OFDM channels," *IEEE Trans. Veh. Technol.*, vol. 66, no. 10, pp. 8795–8806, Oct. 2017.

[26] E. P. Simon *et al.*, "Joint carrier frequency offset and fast time-varying channel estimation for MIMO-OFDM systems," *IEEE Trans. Veh. Technol.*, vol. 60, no. 3, pp. 955–965, Mar. 2011.

[27] J. Qiao, X. S. Shen, J. W. Mark, and L. Lei, "Video quality provisioning for millimeter wave 5G cellular networks with link outage," *IEEE Trans. Wireless Commun.*, vol. 14, no. 10, pp. 5692–5703, Oct. 2015.

[28] C. Chen, R. W. Heath, A. C. Bovik, and G. de Veciana, "A Markov decision model for adaptive scheduling of stored scalable videos," *IEEE Trans. Circuits Syst. Video Technol.*, vol. 23, no. 6, pp. 1081–1095, Jun. 2013.

[29] H. Y. Shen and L. H. Chen, "Distributed autonomous virtual resource management in datacenters using finite-Markov decision process," *IEEE/ACM Trans. Netw.*, vol. 25, no. 6, pp. 3836–3849, Dec. 2017.

[30] E. A. Feinberg and A. Shwartz, Eds., *Handbook of Markov Decision Processes: Methods and Applications.* Dordrecht, The Netherlands, Springer, 2002.

[31] A. J. Goldsmith and P. P. Varaiya, "Capacity, mutual information, and coding for finite-state Markov channels," *IEEE Trans. Inf. Theory*, vol. 42, no. 3, pp. 868–886, May 1996.

[32] A. Fish, S. Gurevich, R. Hadani, A. M. Sayeed, and O. Schwartz, "Delay-doppler channel estimation in almost linear complexity," *IEEE Trans. Inf. Theory*, vol. 59, no. 11, pp. 7632–7644, Nov. 2013.

[33] *Physical Channels and Modulation, V12.6.0*, 3GPP Standard TS 36.211, Jul. 2015.

[34] S. Haykin, *Adaptive Filter Theory*. Englewood Cliffs, NJ, USA: Prentice-Hall, 1996.

[35] J. Ylioinas and M. Juntti, "Iterative joint detection, decoding, and channel estimation in turbo-coded MIMO-OFDM," *IEEE Trans. Veh. Technol.*, vol. 58, no. 4, pp. 1784–1796, May 2009.

[36] Y. E. H. Shehadeh and S. Sezginer, "An iterative channel estimator for fast-varying channels using successive OFDM symbols," in *Proc. IEEE Int. Symp. Pers. Indoor Mobile Radio Commun.*, 2009, pp. 2404–2408.

[37] M. T. Heath, *Scientific Computing: An Introductory Survey*. Boston, MA, USA: McGraw-Hill, 1997.

[38] T. Whitworth, M. Ghogho, and D. McLernon, "Optimized training and basis expansion model parameters for doubly-selective channel estimation," *IEEE Trans. Wireless Commun.*, vol. 8, no. 3, pp. 1490–1498, Mar. 2009.

[39] Z. Tang, R. C. Cannizzaro, G. Leus, and P. Banelli, "Pilot-assisted time-varying channel estimation for OFDM systems," *IEEE Trans. Signal Process.*, vol. 55, no. 5, pp. 2226–2238, May 2007.

[40] D. Slepian, "Prolate spheroidal wave functions, Fourier analysis, and uncertainty—V: The discrete case," *Bell Syst. Tech. J.*, vol. 57, no. 5, pp. 1371–1430, 1978.

[41] G. B. Giannakis and C. Tepedelenlioglu, "Basis expansion models and diversity techniques for blind identification and equalization of time-varying channels," *Proc. IEEE*, vol. 86, no. 10, pp. 1969–1986, Oct. 1998.

[42] D. Guo, S. Shamai, and S. Verdú, "Mutual information and minimum mean-square error in Gaussian channels," *IEEE Trans. Inf. Theory*, vol. 51, no. 4, pp. 1261–1282, Apr. 2005.

[43] D. P. Palomar and S. Verdú, "Representation of mutual information via input estimates," *IEEE Trans. Inf. Theory*, vol. 53, no. 2, pp. 453–470, Feb. 2007.

[44] A. Goldsmith, *Wireless Communications*. Cambridge, U.K.: Cambridge Univ. Press, 2005.

[45] *User Equipment (UE) Radio Transmission and Reception, V11.0.0*, 3GPP Standard TS 36.101, Dec. 2007.

[46] J.-C. Chen, C.-K. Wen, and P. Ting, "An efficient pilot design scheme for sparse channel estimation in OFDM systems," *IEEE Commun. Lett.*, vol. 17, no. 7, pp. 1352–1355, Jul. 2013.

Yan Yang (M'08) was born in Sichuan, China, in 1968. He received the B.Sc. degree in electronics engineering from the University of Electronic Science and Technology of China, Chengdu, China, in 1990, the M.Sc. degree in signal processing from Sichuan University, Chengdu, in 1997, the D.Sc. degree in signal processing from the Institute of Acoustic, Chinese Academy of Science, Beijing, China, in 2004.

From 2014 to 2015, he was a Visiting Scholar with the Georgia Institute of Technology, Atlanta, GA, USA. He is currently an Associate Professor with the State Key Laboratory of Rail Traffic Control and Safety, Beijing Jiaotong University, Beijing. He is an active participant in the Working Party 5A (WP 5A)—Land mobile service conference excluding IMT, amateur and amateur-satellite service, the International Telecommunication Union (ITU) Radiocommunication Sector (ITU-R), and is a Technical Specialist for the research item 1.11 of the Resolution 236 World Radiocommunication Conference (WRC-15). His current research interests include wireless communications, signal processing, and artificial intelligence for cognitive wireless communications.

Dr. Yang was a recipient of the First Research Award from the Science and Technology of China Railways Society in 2007.

Shuping Dang (S'13–M'18) received the B.Eng. (with first class Hons.) degree in electrical and electronic engineering from the University of Manchester, Manchester, U.K., in 2014, the B.Eng. degree in electrical engineering and automation from Beijing Jiaotong University, Beijing, China, in 2014 via a joint "2+2" dual-degree program, and the D.Phil. degree in engineering Science from the University of Oxford, Oxford, U.K., in 2018.

He was also a Certified LabVIEW Associate Developer with National Instrument, Austin, TX, USA, from 2014 to 2016. He is currently a Technical Director with the Research and Development Center, Huanan Communication Company, Ltd., Guangzhou, China. His current research interests include artificial intelligence assisted communications, cooperative communications, wireless signal processing, and 5G communication system design.

Mr. Dang serves as a Reviewer for the IEEE TRANSACTIONS ON WIRELESS COMMUNICATIONS, the IEEE TRANSACTIONS ON COMMUNICATIONS, the IEEE TRANSACTIONS ON COMMUNICATIONS, the IEEE TRANSACTIONS ON VEHICULAR TECHNOLOGY, *Digital Signal Processing* (Springer), the *EURASIP Journal on Wireless Communications and Networking* (Springer), as well as being a TPC member for a number of leading conferences in communication engineering, including IEEE ICC, Globecom, and VTC.

Yejun He (SM'09) received the B.S. degree from the Huazhong University of Science and Technology (HUST), Wuhan, China, in 1994, the M.S. degree in communication and information system from the Wuhan University of Technology, Wuhan, in 2002, and the Ph.D. degree in information and communication engineering from HUST, in 2005.

He is currently a Professor with Shenzhen University, Shenzhen, China, where he is the Director of the Shenzhen Key Laboratory of Antennas and Propagation. He was a Visiting Professor with the University of Waterloo, Waterloo, ON, Canada, and with the Georgia Institute of Technology, Atlanta, GA, USA. His current research interests include channel coding and modulation, MIMO-OFDM wireless communications, space-time processing, energy harvesting communications, and antennas and RF.

Dr. He serves as an Associate Editor of *Security and Communication Networks*. He served as the Technical Program Committee Co-Chair for the Wireless and Optical Communication Conference in 2015. He has served as a Reviewer for various journals, including the IEEE TRANSACTIONS ON VEHICULAR TECHNOLOGY, the IEEE TRANSACTIONS ON COMMUNICATIONS, the IEEE TRANSACTIONS ON INDUSTRIAL ELECTRONICS, and several more. He has also served as the Technical Program Committee Chair or the Session Chair for various conferences, including IEEE GLOBECOM, IEEE ICC, the IEEE Wireless Communications Networking Conference, and the IEEE Vehicular Technology Conference.

Mohsen Guizani (S'85–M'89–SM'99–F'09) received the B.S. degree (with Distinction), M.S. degree in electrical engineering and M.S. and Ph.D. degree in computer engineering from Syracuse University, Syracuse, NY, USA, in 1984, 1986, 1987, and 1990, respectively.

He served as the Associate Vice President of Graduate Studies, Qatar University, Doham Qatar, the Chair of the Computer Science Department, Western Michigan University, Kalamazoo, MI, USA, and the Chair of the Computer Science Department, University of West Florida, Pensacola, FL, USA. He is currently a Professor and the ECE Department Chair with the University of Idaho, Moscow, ID, USA. He also served in academic positions with the University of Missouri–Kansas City, Kansas City, MO, USA, the University of Colorado–Boulder, Boulder, CO, USA, and Syracuse University, Syracuse, NY, USA. His current research interests include wireless communications and mobile computing, computer networks, mobile cloud computing, security, and smart grid.

Dr. Guizani was a recipient of three teaching awards and four research awards throughput his career and the 2017 IEEE Communications Society Recognition Award for his contribution to outstanding research in Wireless Communications. He is currently the Editor-in-Chief of *IEEE Network Magazine*, serves on the Editorial Boards of several international technical journals and is the founder and the Editor-in-Chief of *Wireless Communications and Mobile Computing Journal* (Wiley). He has authored nine books and over 500 publications in refereed journals and conferences. He guest edited a number of special issues in IEEE journals and magazines. He also served as a member, the Chair, and the General Chair of a number of international conferences. He was the Chair of the IEEE Communications Society Wireless Technical Committee and the Chair of the TAOS Technical Committee. He served as the IEEE Computer Society Distinguished Speaker from 2003 to 2005. He is a Senior Member of the ACM.